Correlating the Crystallization Kinetics of Syndiotactic Polystyrene

C. A. Hieber

138 Upson Hall, Sibley School of Mechanical and Aerospace Engineering, Cornell University, Ithaca, New York 14853-7501

Received 21 January 2003; accepted 23 May 2003

ABSTRACT: The Nakamura equation is used to model the crystallization kinetics of syndiotactic polystyrene. Model constants are generated by fitting available data under isothermal conditions. The resulting fit is then applied to available data under constant-cooling-rate conditions, with notable agreement provided the measurements include corrections for thermal lag. © 2003 Wiley Periodicals, Inc. J Appl Polym Sci 91: 2402–2406, 2004

Key words: crystallization; kinetics; polystyrene; syndiotactic

INTRODUCTION

Syndiotactic polystyrene (sPS), a fairly recently developed polymer[1,2] which exhibits enhanced properties and excellent processibility, has been receiving considerable attention. In the present article, consideration is given to available cumulative data concerning the crystallization kinetics of sPS under isothermal[3–7] as well as nonisothermal[4,7–10] conditions. Making use of the Nakamura[11] model, which includes the Avrami[12] limit (under isothermal conditions) and the Ozawa[13] limit (under constant-cooling/heating-rate conditions), a correlation is developed which describes the cumulative data very well and clearly demonstrates the need to correct for thermal lag in the case of nonisothermal DSC measurements at high cooling/heating rate.

KINETICS MODELING

Under isothermal conditions, the time-dependent relative crystallinity according to the Avrami[12] model is given by

$$\chi = 1 - \exp\{-k(T)t^n\} \tag{1}$$

where $k(T)$ is the temperature-dependent Avrami rate constant and n is the Avrami index, typically lying between 2 and 4. Analogously, the Ozawa[13] model for the case of constant cooling rate is given by

$$\chi = 1 - \exp\left\{-\frac{\kappa(T)}{\varphi^n}\right\} \tag{2}$$

where $\kappa(T)$ is the Ozawa rate constant and $\varphi \equiv -dT/dt$ is the constant cooling rate.

More generally, for the case of arbitrary thermal history, the Nakamura[11] model is given by

$$\chi = 1 - \exp\left\{-\left[\int_0^t K(T)dt\right]^n\right\} \tag{3}$$

In particular, (3) is seen to reduce to (1) under isothermal conditions provided that

$$K^n(T) = k(T) \tag{4}$$

whereas (3) reduces to (2) under constant cooling rate, when

$$dt = -\frac{dT}{\varphi} \tag{5}$$

provided that

$$\left[\int_T^{T_i} K(\tilde{T})d\tilde{T}\right]^n = \kappa(T) \tag{6}$$

where T_i denotes the initial temperature taken sufficiently high above the melting temperature, T_m, where the rate constant is vanishingly small.

In dealing with the above models, it is convenient to introduce the following variables:[14]

Correspondence to: C. A. Hieber (cah31@cornell.edu).

Journal of Applied Polymer Science, Vol. 91, 2402–2406 (2004)

TABLE I
Experimental Investigations[3–7] Related to Isothermal Crystallization of sPS

Source	Ref. no.	$\bar{M}_w$	$\bar{M}_w/\bar{M}_n$	T (°C)	n
Cimmino et al. (1991)	3	710K	3.1	125–140	2.97
				240–250	3.31
St. Lawrence and Shinozaki (1997)	4	372K		122–132	(3.23, 3.36)
				244–252	(2.69, 2.72)
Chiu et al. (2001)	5	356K	1.62	236–252	(3.7, 5.1)
Duff et al. (2001)	6	162K		238–252	
		292K		232–250	(2.36, 2.76)
		400K		236–248	
Chen et al. (2002)	7	220K	2.4	236–244	(1.1, 2.0)

$$\lambda(T) \equiv k^{-1/n}(T) = K^{-1}(T) \tag{7}$$

and

$$\sigma(T) \equiv \kappa^{1/n}(T) \tag{8}$$

Accordingly, from (6), (7), and (8), it follows that

$$\sigma(T) = \int_T^{T_i} \frac{d\tilde{T}}{\lambda(\tilde{T})} \tag{9}$$

where $\lambda(T)$ is the characteristic time of the kinetics.

In modeling the temperature dependence of the various parameters above, one might follow Sifleet et al.,[15] who used a quadratic fit for $\ln[k(T)]$. Equivalently, Ziabicki[16] employed a Gaussian functional form for $k(T)$ itself. By using the latter representation, as applied to $\lambda(T)$ in (7), we set

$$\lambda(T) = \lambda_{\min} \exp\left\{\left(\frac{T - T_{\min}}{D}\right)^2\right\} \tag{10}$$

where $\lambda_{\min}$, $T_{\min}$, and D are model constants. It is noted that (10) has been employed previously[17] under more general conditions, namely the injection molding of isotactic polypropylene, where $T_{\min}$ has been taken to be pressure dependent and D has been taken to be dependent upon the flow-induced shear stress.

Making use of (9) and (10), it then follows that

$$\sigma(T) = \frac{D}{\lambda_{\min}} \tilde{\sigma}(\xi) \tag{11}$$

where

$$\xi \equiv \frac{T - T_{\min}}{D} \tag{12}$$

and

$$\tilde{\sigma}(\xi) = \int_\xi^\infty e^{-u^2} du \equiv \frac{\sqrt{\pi}}{2} \operatorname{erfc}(\xi) \tag{13}$$

That is, (11)–(13) define the Ozawa rate constant in (2, 8) once the ($\lambda_{\min}$, $T_{\min}$, D) parameters in (10), defining the Avrami rate constant in (1, 7), have been determined. It is noted that $\sigma(T)$ had been generated from $\lambda(T)$ elsewhere[14] by numerically solving a first-order differential equation. Based on (11)–(13), $\sigma(T)$ has now been determined from $\lambda(T)$ in terms of a closed-form relation.

ISOTHERMAL-CRYSTALLIZATION RESULTS

Listed in Table I are available experimental results from the literature[3–7] relating to the crystallization of sPS under isothermal conditions. All these bulk-crystallization results are based upon differential scanning calorimetry (DSC). In two instances,[3,4] it is noted that cold-crystallization results have also been obtained, involving a thermal quench to below the glass-transition temperature (T_g) before quickly raising the temperature to the particular level of interest (such as 125–140°C in the case of Cimmino et al.[3]). The last column in Table I indicates the reduced experimental values for the Avrami index, n in (1), which is seen to typically lie in the range between 2 and 4, although anomalously lower in the case of Chen et al.[7] and somewhat higher in Chiu et al.[5]

Making use of the isothermal crystallization data[3–7] in terms of $t_{1/2}(T)$, namely the time at which $\chi = 0.5$ in (1), and noting from (1) and(7) that

$$\lambda(T) = \frac{t_{1/2}(T)}{(\ell n 2)^{1/n}} \tag{14}$$

corresponding experimental results are shown plotted in Figure 1. In particular, it is quite reassuring that the cold-crystallization results, limited to only two sources,[3,4] are in very good mutual agreement despite the added difficulty of such measurements.

The dashed curve in Figure 1 is the corresponding best fit of the cumulative data points based upon (10) with

$$(\lambda_{\min}, T_{\min}, D) = (0.8293\ \text{s}, 188.6°\text{C}, 24.66°\text{C}) \quad (15)$$

which fits the points with a root-mean-square (rms) deviation of 37.3%. In comparing the dashed curve with the data points in Figure 1, it is noted that, other than two points from Chen et al.,[7] the only data points lying below the dashed curve in Figure 1(b) are due to Duff et al.[6] Accordingly, the dashed curve seems to be skewed by the latter data points. (Part of the reason could be due to the fact that the open square data points in Fig. 1 correspond to the lowest $\bar{M}_w$ of all the resins in Table I. On the other hand, the 292K and 400K molecular-weight data points[6] also lie generally low relative to the dashed curve.) In particular, if we omit all the data points from Duff et al.,[6] the resulting best fit based upon (10) corresponds to

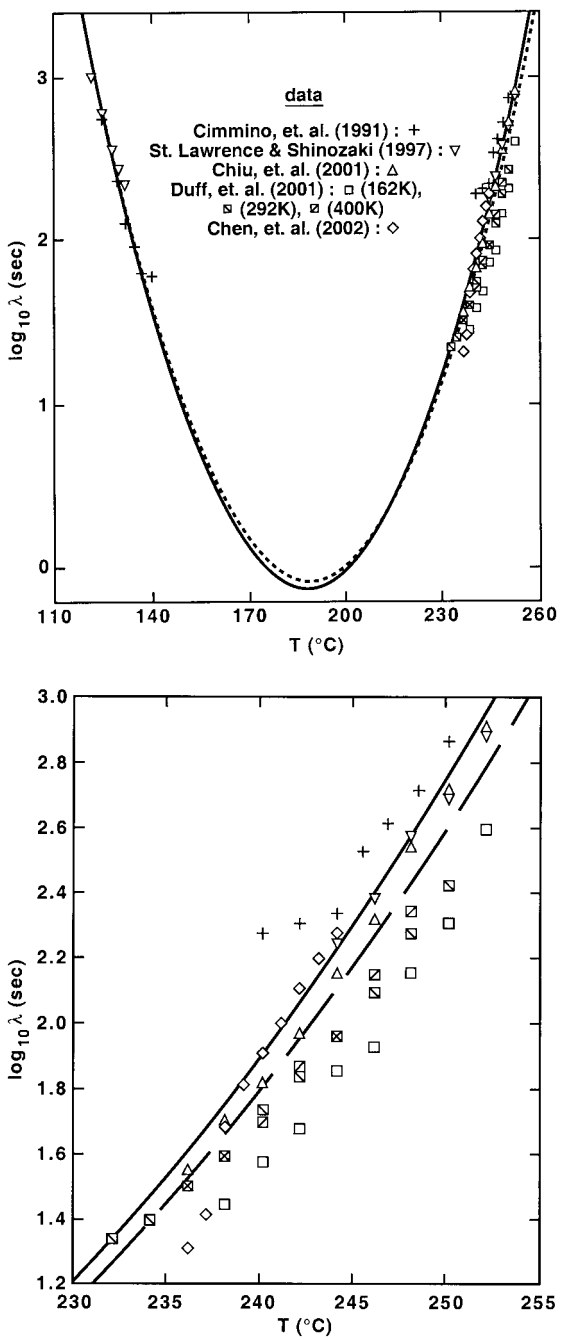

Figure 1 (a) Experimental results (symbols) for $\lambda(T)$ based upon isothermal crystallization data for sPS from the five sources listed in Table I. Dashed and solid curves are best fits corresponding to (10, 15) and (10, 16), respectively, as documented in text. (b) Expanded view of a portion of (a).

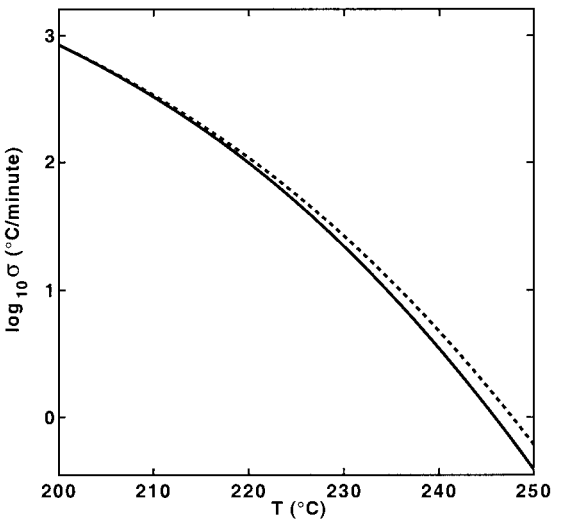

Figure 2 Curves for $\sigma(T)$ based upon (11)–(13) with dashed curve corresponding to (15) and solid curve corresponding to (16).

$$(\lambda_{\min}, T_{\min}, D) = (0.7487\ \text{s}, 187.8°\text{C}, 24.11°\text{C}) \quad (16)$$

with an rms deviation of 27.2% for the cumulative data points from the remaining four investigations.[3–5,7]

CONSTANT-COOLING-RATE CRYSTALLIZATION RESULTS

Based upon the above values for $(\lambda_{\min}, T_{\min}, D)$ in (15) and (16), we can plot results for $\sigma(T)$, related to the Ozawa rate constant via (8), by making use of (11)–(13). Such results are shown plotted in Figure 2.

Furthermore, if $T_{1/2}$ denotes the temperature at which $\chi = 0.5$ under constant-cooling rate φ, then it follows from (2) and (8) that

$$\sigma(T_{1/2}) = (\ell n 2)^{1/n} \varphi \quad (17)$$

Hence, with $\sigma(T)$ known from Figure 2, we can make use of (17) to then plot $T_{1/2}$ versus φ, which is indicated in Figure 3, using $n = 3$ in (17). [It might be noted that the factor $(\ln 2)^{1/n}$ depends only weakly on

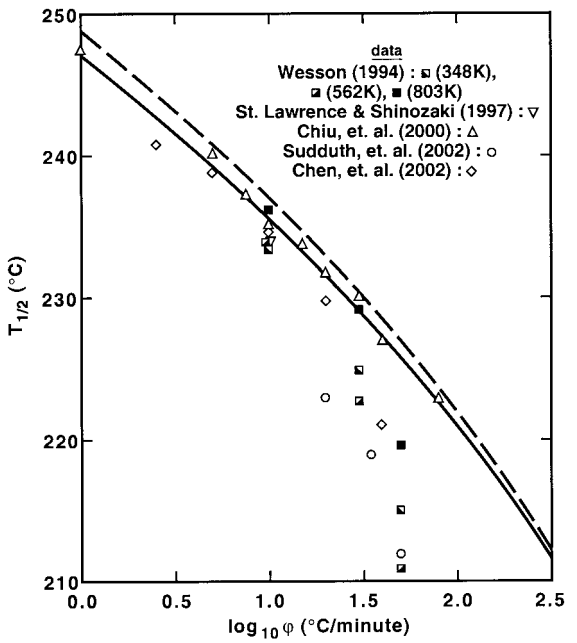

Figure 3 Results for $T_{1/2}$ versus φ. Solid and dashed curves correspond to respective curves in Figure 2, making use of (17) with $n = 3$. Symbols are experimental results for constant-cooling-rate crystallization data for sPS from the five sources listed in Table II.

n, changing by only 10% as n varies between 2 and 4.] That is, for a given value of $T_{1/2}$ in Figure 3, we determine $\sigma(T_{1/2})$ from Figure 2 and then use (17) to determine φ, as then employed in Figure 3.

Also indicated in Figure 3 are experimental results for $T_{1/2}$ versus φ from five sources in the literature,[4,7–10] as documented in Table II. In particular, it is noted that the nine data points (Δ) from Chiu et al.[9] agree extremely well with the solid curve in Figure 3, with an rms deviation of 0.5°C over the extensive cooling-rate range of 1 to 80°C/min. On the other hand, it is noted that the bulk of the remaining data in Figure 3 lies systematically below the solid curve, particularly at the higher cooling rates.

In addressing the above discrepancy, it is noted that of the five experimental investigations[4,7–10] reported in Figure 3, only Chiu et al.[9] corrected their data for the effects of thermal lag. Although results for their own experimentally determined thermal–lag correction are not explicitly presented by Chiu et al.,[9] one might refer to earlier work by Monasse and Haudin,[18] dealing with polypropylene, in which the thermal–lag correction was determined experimentally and fitted with a linear dependence upon cooling rate, namely

$$\Delta T_{\text{corr}} = C\varphi, \quad C = 0.107 \text{ min} \tag{18}$$

According to this result, the actual specimen temperature would be higher than the instrument reading by 1.07°C at $\varphi = 10$°C/min and by 10.7°C at $\varphi = 100$°C/min. In turn, such results are seen to be of the same order of magnitude as the systematic deviation below the solid curve of the uncorrected data[8,4,10,7] in Figure 3. Accordingly, these results seem to dramatically indicate the need to correct constant-cooling-rate DSC data for thermal lag at the higher cooling rates. Furthermore, by means of the solid curves in Figures 1 and 3, it follows that the isothermal data in Figure 1 are consistent with the constant-cooling-rate data in Figure 3, when the latter are corrected for thermal lag. In turn, it follows that the present modeling, with one set of model constants [as given in eq. (16)], can describe both isothermal and constant-cooling-rate data for sPS.

DISCUSSION

Although not included in the preceding section, it is noted that St. Lawrence and Shinozaki[4] also did cold-crystallization measurements at a constant-heating rate, namely $\varphi = -10$°C/min, as indicated in Table II. In this case, their experimental value for $T_{1/2}$ is 138.1°C.

To apply the current fit to the constant-heating-rate case, it is noted that the present proposed correlation in terms of (3, 7, 10, 16) is symmetric with respect to T_{min} in (10). Hence, because the present correlation given by the solid curve in Figure 3 gives a $T_{1/2}$ at $\varphi = 10$°C/min of 235.5°C, i.e., $T_{1/2} - T_{\text{min}} = 235.5$°C $- 187.8$°C $= 47.7$°C, then $T_{1/2}$ at $\varphi = -10$°C/min will occur at 47.7°C below T_{min}, namely at 187.8°C

TABLE II
Experimental Investigations[8,4,9,10,7] Related to Nonisothermal Crystallization of sPS

Source	Ref. no.	$\bar{M}_w$	$\bar{M}_w/\bar{M}_n$	φ (°C/min)
Wesson (1994)	8	348K		10, 30, 50
		562K		10, 30, 50
		830K		10, 30, 50
St. Lawrence and Shinozaki (1997)	4	372K		−10, 10
Chiu et al. (2000)	9	356K	1.62	1, 5, 7.5, 10, 15, 20, 30, 40, 80
Sudduth et al. (2002)	10	244K		20, 35, 50
Chen et al. (2002)	7	220K	2.4	2.5, 5, 10, 20, 40

− 47.7°C = 140.1°C. It is seen that this result lies within 2°C of the experimental value, which seems to be quite reasonable.

Of course, if we correct the above experimental value of 138.1°C for thermal lag, the actual value should be lower, thus worsening the comparison with the predicted value of 140.1°C. Making use of the results at φ = 10°C/min in Figure 3, as well as the experimental findings of Monasse and Haudin[18] as given in (18), one might expect the thermal lag at φ = −10°C/min to be also ~ 1°C. However, if one refers to investigations[19–22] that deal with modeling the thermal lag in DSC measurements, there is reason to conclude that the thermal–lag effect will actually be smaller in the constant heating mode. This is due to the fact that part of the lag is due to the heat source arising from the crystallization effect, which tends to raise the actual temperature of the specimen and thus actually diminishes the amount by which the specimen temperature lags behind the imposed furnace temperature in the constant-heating-rate case.

It is also of interest to note that the present results do agree quite well with the empiricism[23] that the maximum rate of crystallization occurs approximately midway between T_g and T_m. Specifically, for PS we have that $T_g \approx 100$°C,[24] whereas for sPS, $T_m \approx 270$°C[1] such that the average value of T_g and T_m is closely approximated by the value of $T_{\min}$ = 187.8°C in (16).

In summary, the present proposed correlation for the crystallization kinetics of sPS is based upon the Nakamura model, as defined by eqs. (3, 7, 10, 16) and plotted as the solid curves in Figures 1–3 (using a representative value for n of 3, in Fig. 3). For the isothermal-crystallization results in Figure 1, the solid curve is seen to fit the cumulative data from four of the five sources quite well. As then applied to constant-cooling-rate results in Figure 3, the solid curve is seen to agree extremely well with the data of Chiu et al.[9] over the extensive range of φ between 1 and 80°C/min. Whereas this data set was corrected for thermal–lag effects, the other four sources of experimental results plotted in Figure 3 were not corrected for this effect and thus lie systematically low, particularly at the higher cooling rates. When combined with the findings of Monasse and Haudin,[18] the results in Figure 3 serve as a clear indication of the need to correct constant-cooling-rate data for thermal–lag effects at higher values of φ. Furthermore, the combined results in Figures 1 and 3 confirm the ability of the Nakamura model (with one set of model constants) to describe both isothermal and nonisothermal crystallization data for sPS. In addition, in a manner similar to elsewhere,[14,17,25] the present results also imply that there is no need to explicitly incorporate an induction time into the modeling.

References

1. Ishihara, N.; Seimiya, T.; Kuramoto, M.; Uoi, M. Macromolecules 1986, 19, 2464.
2. Pellecchia, C.; Longo, P.; Grassi, A.; Ammendola, P.; Zambelli, A. Makromol Chem, Rapid Commun 1987, 8, 277.
3. Cimmino, S.; Di Pace, E.; Martuscelli, E.; Silvestre, C. Polymer 1991, 32, 1080.
4. St. Lawrence, S.; Shinozaki, D. M. Polym Eng Sci 1997, 37, 1825.
5. Chiu, F.-C.; Shen, K.-Y.; Tsai, S. H. Y.; Chen, C.-M. Polym Eng Sci 2001, 41, 881.
6. Duff, S.; Tsuyama, S.; Iwamoto, T.; Fujibayashi, F.; Birkinshaw, C. Polymer 2001, 42, 991.
7. Chen, Q.; Yu, Y.; Na, T.; Zhang, H.; Mo, Z. J Appl Polym Sci 2002, 83, 2528.
8. Wesson, R. D. Polym Eng Sci 1994, 34, 1157.
9. Chiu, F.-C.; Peng, C.-G.; Fu, Q. Polym Eng Sci 2000, 40, 2397.
10. Sudduth, R. D.; Yarala, P. K.; Sheng, Q. Polym Eng Sci 2002, 42, 694.
11. Nakamura, K.; Watanabe, T.; Katayama, K.; Amano, T. J Appl Polym Sci 1972, 16, 1077; 1973, 17, 1031.
12. Avrami, M. J Chem Phys 1939, 7, 1103; 1940, 8, 212.
13. Ozawa, T. Polymer 1971, 12, 150.
14. Hieber, C. A. Polymer 1995, 36, 1455.
15. Sifleet, W. L.; Dinos, N.; Collier, J. R. Polym Eng Sci 1973, 13, 10.
16. Ziabicki, A. Fundamentals of Fibre Formation; Wiley: London, 1976; Chapter 2.
17. Hieber, C. A. Polym Eng Sci 2002, 42, 1387.
18. Monasse, B.; Haudin, J. M. Colloid Polym Sci 1986, 264, 117.
19. Janeschitz-Kriegl, H.; Wippel, H.; Paulik, Ch.; Eder, G. Colloid Polym Sci 1993, 271, 1107.
20. Wu, C. H.; Eder, G.; Janeschitz-Kriegl, H. Colloid Polym Sci 1993, 271, 1116.
21. Chan, T. W.; Shyu, G. D.; Isayev, A. I. SPE ANTEC Tech Papers 1994, 40, 1480.
22. Chan, T. W.; Isayev, A. I. Polym Eng Sci 1994, 34, 461.
23. Van Krevelen, D. W. Properties of Polymers, 3rd ed.; Elsevier Science: Amsterdam, 1990; p 594.
24. Van Krevelen, D. W. Properties of Polymers, 3rd ed.; Elsevier Science: Amsterdam, 1990; p 792.
25. Hieber, C. A. Int Polym Process 1997, 12, 249.